Amino Acids (2011) 40:205–214
DOI 10.1007/s00726-010-0635-y

ORIGINAL ARTICLE

Adsorption of cysteine on hematite, magnetite and ferrihydrite: FT-IR, Mössbauer, EPR spectroscopy and X-ray diffractometry studies

Alessandra P. Vieira · Graciele Berndt · Ivan G. de Souza Junior · Eduardo Di Mauro · Andrea Paesano Jr · Henrique de Santana · Antonio Carlos S. da Costa · Cássia T. B. V. Zaia · Dimas A. M. Zaia

Received: 29 April 2010 / Accepted: 15 May 2010 / Published online: 4 June 2010

Abstract In the present paper, the adsorption of cysteine on hematite, magnetite and ferrihydrite was studied using FT-IR, electron paramagnetic resonance (EPR), Mössbauer spectroscopy and X-ray diffractometry. Cysteine was dissolved in artificial seawater (two different pHs) which contains the major constituents. There were two main findings described in this paper. First, after the cysteine adsorption, the FT-IR spectroscopy and X-ray diffractometry data showed the formation of cystine. Second, the Mössbauer spectroscopy did not show any increase in the amount of Fe^{2+} as expected due the oxidation of cysteine to cystine. An explanation could be that Fe^{2+} was oxidized by the oxygen present in the seawater or there occurred a reduction of cystine by Fe^{2+} generating cysteine and Fe^{3+}. The specific surface area and pH at point of zero charge of the iron oxides were influenced by adsorption of cysteine. When compared to other iron oxides, ferrihydrite adsorbed significantly ($p < 0.05$) more cysteine. The pH has a significant ($p < 0.05$) effect only on cysteine adsorption on hematite. The FT-IR spectroscopy results showed that cystine remains adsorbed on the surface of the iron oxides even after being mixed with KCl and the amine and carboxylic groups are involved in this interaction. X-ray diffractometry showed no changes on iron oxides mineralogy and the following precipitated substances were found along with the iron oxides after drying the samples: cysteine, cystine and seawater salts. The EPR spectroscopy showed that cysteine interacts with iron oxides, changing the relative amounts of iron oxides and hydroxide.

Keywords Iron oxides · Amino acids · Surface complexation · Spectroscopy · Prebiotic chemistry

A. P. Vieira · H. de Santana · D. A. M. Zaia (✉)
Departamento de Química-CCE, Universidade Estadual de Londrina, Londrina, PR 86051-990, Brazil
e-mail: damzaia@uel.br

G. Berndt · A. Paesano Jr
Departamento de Física-CCE, Universidade Estadual de Maringá, Maringá, PR 87020-900, Brazil

I. G. de Souza Junior · A. C. S. da Costa
Departamento de Agronomia-CCA, Universidade Estadual de Maringá, Maringá, PR 87020-900, Brazil

E. Di Mauro
Laboratório de Fluorescência e Ressonância Paramagnética Eletrônica (LAFLURPE)-CCE, Universidade Estadual de Londrina, Londrina, PR 86051-990, Brazil

C. T. B. V. Zaia
Departamento de Ciências Fisiológicas-CCB, Universidade Estadual de Londrina, Londrina, PR 86051-990, Brazil

Introduction

Since Bernal (1951) suggested that minerals could play an important role in origin of life on Earth, because they participated in the concentration of biomolecules from dilute solution as well as in the formation of biopolymers, several experiments have been carried out to test this hypothesis. The adsorption of amino acids on minerals is an important issue from prebiotic chemistry point of view since most of the reactions of the living beings involve amino acids/peptides/proteins (Darnell et al. 1990). Several good reviews related to the adsorption of amino acids on minerals appear in the literature (Lahav and Chang 1976; Basiuk 2002; Zaia 2004; Lambert 2008).

As reviewed by Zaia et al. (2008), cysteine could be synthesized under conditions that simulate prebiotic atmospheres and hydrothermal vents. Iron is the fourth most abundant element in the crust of Earth. Thus, the reactions and the compounds of this metal are very important in several fields of science and technology such as metallurgy, pure chemistry, medicine, industrial chemistry, soil science and environmental science. For all iron oxides the basic structural unit is octahedron, where each Fe atom is surrounded by six O or OH ions (Schwertmann and Cornell 1991). Iron oxides are widespread in nature and can be found in soils, rocks, lakes, rivers, sea floor and living organisms (Schwertmann and Cornell 1991; Wade et al. 1999; Bishop and Murad 2002) as well as in meteorites, on the surface of Mars and in interplanetary dust particles (Rietmeijer 1996; Catling and Moore 2003; Faivre and Zuddas 2006). Thus, cysteine and iron oxides are substances that could be easily found on the prebiotic Earth.

The adsorption of cysteine on several minerals has been studied such as pyrite (Bebié and Schoonen 2000), clays (Brigatti et al. 1999; Benetoli et al. 2007; de Santana et al. 2010), silica (Basiuk and Gromovoy 1996; Basiuk 2002) and metals (Stewart and Fredericks 1999; Marti et al. 2004; Aryal et al. 2006). In general, the adsorption of cysteine on minerals is due to the interactions of cysteine/metals. Besides, cysteine has three functional groups (thiol, amine, carboxylic) that can interact with minerals. The thiol group involved in these interactions can be easily identified by FT-IR, where the stretching S–H band at 2,562 cm^{-1} vanishes (Bebié and Schoonen 2000; Aryal et al. 2006; Benetoli et al. 2007; de Santana et al. 2010). However, in some cases the amine and/or carboxylic groups may also be involved (Brigatti et al. 1999; Stewart and Fredericks 1999; Benetoli et al. 2007).

Several authors have studied the role of cysteine as well as thioglycolicacid in the dissolution (Baumgartner et al. 1982; Amirbahman et al. 1997; Doong and Schink 2002) or formation (Cohen et al. 2008; Mantion et al. 2008) processes of iron oxides. The dissolution of iron oxides by cysteine is a complex mechanism that involves the formation of cystine as well as the participation of free radicals (Amirbahman et al. 1997; Doong and Schink 2002). According to Mantion et al. (2008), cysteine prevents the formation of magnetite. Cohen et al. (2008) described the synthesis of Fe_3O_4 nanoparticles capped with DL-cysteine as well as the formation of cystine.

The present paper describes the interaction as well as the adsorption of cysteine on hematite, ferrihydrite and magnetite at two different pH values. The interaction of cysteine with hematite, ferrihydrite, and magnetite was studied using FT-IR, electron paramagnetic resonance (EPR), Mössbauer spectroscopy and X-ray diffractometry. It should be pointed out that as far as we know there are no studies of the adsorption of cysteine on iron oxides.

Materials and methods

Materials

All reagents were of analytical grade.

Iron oxides (hematite, ferrihydrite, magnetite)

Iron oxides were synthesized as described by Schwertmann and Cornell (1991).

Artificial seawater

The following substances were weighed and dissolved in 1.0 L of distilled water: 28.57 g of sodium chloride, 3.88 g of magnesium chloride, 1.787 g of magnesium sulfate, 1.308 g of calcium sulfate, 0.832 g of potassium sulfate, 0.124 g of calcium carbonate, 0.103 g of potassium bromide and 0.0282 g of boric acid.

Sample preparation

Cysteine was dissolved in artificial seawater at concentrations of 0.72 and 24.2 mg mL^{-1}. Each iron oxide (hematite, ferrihydrite, magnetite) was processed as follows: to three different sets of four tubes (15 mL) containing 100 mg of iron oxide (hematite, ferrihydrite, magnetite) were added: (1) 5.00 mL of artificial seawater, (2) 5.00 mL of artificial seawater with 0.72 mg mL^{-1} of cysteine and (3) 5.00 mL of artificial seawater with 24.2 mg mL^{-1} of cysteine. The pH was adjusted to 3.00 or 7.20 with HCl or NaOH. The tubes were mixed for 24 h, after which they were spun for 15 min at 2,000 rpm. The aqueous phase of the tubes with concentration of 0.72 mg mL^{-1} of cysteine was used for the measurement of the amount of cysteine adsorbed on iron oxides and the solid was discharged. The aqueous phase of the tubes with concentration of 24.2 mg mL^{-1} was lyophilized and used for FT-IR spectroscopy and the solids were dried in an oven at 60°C for 24 h. A portion of dried solids was used for FT-IR, EPR, Mössbauer spectroscopy and X-ray diffractometry. Another portion of the dried solids was transferred to 15 mL tubes and 5.00 mL of 0.20 mol L^{-1} KCl was added. The tubes were mixed for 24 h, and later spun for 15 min at 2,000 rpm. The aqueous phase was again lyophilized and used for FT-IR spectroscopy. The solids were dried overnight in an oven at 60°C and used for FT-IR and EPR spectroscopy.

Methods

Specific surface area of iron oxides

Specific surface area values were measured using a Quantachrome—Quantasorb Surface Area Analyser by the adsorption of N_2 and the areas were calculated using Brunauer–Emmett–Teller method (Brunauer et al. 1938).

Visible spectrophotometric method

Cysteine was determined using the *p*-benzoquinone method as described by Zaia et al. (1999).

Infrared spectroscopic method

The IR spectra were recorded with a FT-IR 8300 Shimadzu using pressed KBr disks and a spectral resolution of 4 cm^{-1}, and each spectrum was obtained after acquiring 85 spectra. FT-IR analysis was carried out with iron oxides samples, with and without cysteine adsorption, as well as lyophilized samples and iron oxides that were mixed with KCl. About 10 mg of iron oxide or lyophilized samples plus 200 mg of KBr were weighed and ground in an agate mortar with a pestle until a homogeneous mixture was obtained. Disc pellets were prepared and spectra were recorded from 400 to 4,000 cm^{-1}. FT-IR spectra were analyzed by the Origin program (5.0, 2001).

Electron paramagnetic resonance spectroscopy method

The samples were submitted to EPR experiment at X-band (ca. 9 GHz) with 20 G modulation amplitude and a magnetic field modulation of 100 kHz using a JEOL (JES-PE-3X) spectrometer at room temperature. Mn^{2+}:MgO was used as *g* marker and standard of line intensity, using its fourth spectrum line ($g = 1.981$).

Mössbauer spectroscopy method

Mössbauer spectroscopy characterizations were performed in transmission geometry, using a conventional Mössbauer spectrometer, in a constant acceleration mode. The γ-rays were provided by a ^{57}Co(Rh) source, with initial nominal activity of 50 mCi. The Mössbauer spectra were analyzed with a nonlinear least-square routine, with Lorentzian line shapes. All isomer shift (IS) data given are relative to α-Fe throughout this paper.

X-ray diffractometry method

The X-ray diffractograms were obtained in an XRD-6000 Shimadzu, using Cu Kα, a monochromator, and the scanning parameters were set at 0.02°2θ, step width, count time 0.6 s and a measurement range from 2 to 30°2θ. The powder samples were placed on a glass slide. X-ray diffractograms were analyzed by Grams/386 v 4.0 (Galactic Ind. Corp.) software.

Statistical analysis

Comparisons between means were assessed by using ANOVA and Student–Newman–Keuls test (SNK test) at a significance level of $p < 0.05$.

Results and discussion

Table 1 shows pH at point of zero charge and specific surface area values of the iron oxides (hematite, ferrihydrite, magnetite) with and without cysteine adsorbed on them. The pH at point of zero charge values are in good agreement with those of Kosmulski et al. (2003) and these values could vary in a wide range (from almost 3.00 to more than 10.0); however, most of pH at point of zero charge values are in the 5.00–9.50 range. The pH at point of zero charge values of iron oxides with previous treatment (artificial seawater, artificial seawater plus cysteine) showed variation when compared to those without previous treatment and these variations were more effective for the pH 7.0 treatment (Table 1). For some treatments, an increase in pH at point of zero charge values was observed

Table 1 pH at point of zero charge and specific surface area of hematite, ferrihydrite and magnetite

Iron oxide	Sample	Range of pH	pH_{pcz}*	SSA ($m^2\ g^{-1}$)**
Hematite	Without Cys	2.36–3.63	4.80	5.1
	With Cys		4.26	6.9
	Without Cys	6.74–7.49	6.20	5.3
	With Cys		7.40	6.1
Ferrihydrite	Without Cys	4.51–4.78	5.84	123.9
	With Cys		6.06	50.6
	Without Cys	5.56–6.06	4.73	109.7
	With Cys		4.73	29.5
Magnetite	Without Cys	2.91–4.05	4.21	19.3
	With Cys		4.34	14.5
	Without Cys	4.87–6.15	5.21	17.5
	With Cys		8.09	15.0

* pH at point of zero charge was calculated using the equation: $pH_{pzc} = 2$ pH (1.0 mol L^{-1} KCl) − pH (distilled water) Uehara (1979). pH at point of zero charge of hematite, ferrihydrite and magnetite without previous treatment were: 4.43, 5.78 and 4.62, respectively

** Specific surface areas of iron oxides without previous treatment were 7.8 (hematite), 179.2 (ferrihydrite) and 23.8 (magnetite) $m^2\ g^{-1}$

while an opposite trend was observed for others. Polyprotic acid such as phosphate (Li and Stanforth 2000) and soil humus Baalousha (2009) usually promote a decrease in pH at point of zero charge due to its capacity of dissociating protons and the predominance of negative charge on surface functional groups, respectively. Otherwise, the formation of inner-sphere complexes between the iron oxides' surface functional group with metal cations, by cation bridges and ligand exchange with other surface functional groups with pKa in the alkaline range, might create positive charge on the iron oxides' surface increasing their pH at point of zero charge (Sposito 1989).

The specific surface area of iron oxides decreased when the samples were treated with artificial seawater or artificial seawater plus cysteine (Table 1). For ferrihydrite and magnetite the decrease of specific surface area was more pronounced in the mixed samples treated with artificial seawater plus cysteine than in those solely treated with artificial seawater. An opposite trend was observed for hematite (Table 1). Among the iron oxides studied, ferrihydrite has the highest specific surface area and it showed the highest decrease in specific surface area after treatment with a solution of artificial seawater or artificial seawater plus cysteine (Table 1). The decrease of specific surface area of iron oxides is related to precipitation of artificial seawater salts (Halite) adsorbed to the external surfaces and entrapped in the pores among particles, after drying (Fig. 1). Therefore, magnetite and ferrihydrite, with greater specific surface area, retained more sea salts than hematite and had a more pronounced decrease in the specific surface area due to dilution of the original sample.

Table 2 shows the amount of cysteine adsorbed on iron oxides in two different ranges of pH, the net charge of iron oxides and cysteine. Based on the pH at point of zero charge values (Table 1) and pH range (Table 2), hematite and magnetite have positive net charge. Ferrihydrite has negative net charge at higher range of pH and the net charge could be positive or negative at lower range of pH. Based on pH range values (Table 2) and pH at isoelectric point of cysteine (5.07), at lower pH range ($pH < 5$) the surface functional groups are protonated and attribute positive charge (Table 2) to minerals. This was more pronounced for the hematite and magnetite at the low pH range treatments. For the pH values above 5, the carboxylic surface functional group ($pK_a \approx 5.0$) become more negative while the thiol and amino groups ($pK_a > 9.0$) remain protonated and attribute positive charge to the iron oxides. Ferrihydrite showed the highest adsorption of cysteine when compared to hematite and magnetite ($p < 0.05$) (Table 2). For ferrihydrite, for pH values above 5.5, the net charge is negative and associated to the highest surface area and amount of cysteine adsorbed that neutralized most of the protonated thiol and amine surface functional groups, creating negative charge with the deprotonated carboxylic ones. Therefore, more net negative charge is created on the iron oxides' surfaces as pH increases and more cysteine is adsorbed. For magnetite, we observed a bigger adsorption at higher range of pH than lower range, however, the adsorption was not statically different from each other ($p > 0.05$) (Table 2). Matrajt and Blanot (2004) also observed same results when they studied the adsorption of aspartic and glutamic acids (negative net charge) on ferrihydrite (positive net charge). According to the authors, those amino acids were totally adsorbed on ferrihydrite but other amino acids not. Amirbahman et al. (1997) and Doong and Schink (2002) observed that pH had an effect on adsorption of cysteine on Fe^{3+} (hydroxyl) oxides. Otherwise, Benetoli et al. (2007) studied the adsorption of cysteine on kaolinite and bentonite in three different range of pH (3.00, 6.00, 8.00), and observed no effect on the adsorption of cysteine on both minerals. Ferrihydrite showed the highest adsorption of cysteine compared to hematite and magnetite ($p < 0.05$) (Table 2). This higher adsorption is probably due to the highest specific surface area of ferrihydrite compared to hematite and magnetite (Table 1). Brigatti et al. (1999) observed that the amount of cysteine adsorbed on smectites depends on the cation in the interlayer of the mineral. Basiuk and Gromovoy (1996) and Basiuk (2002) studied the adsorption of several amino acids on silica. According to them, the adsorption of cysteine on silica was higher than other amino acids because the sulfide group of cysteine noticeably decreases adsorption $\Delta G°$. However, Benetoli et al. (2007) did not observe variation of the amount of cysteine adsorbed on bentonite and kaolinite.

In order to better understand the interaction between cysteine and the iron oxides (hematite, magnetite, ferrihydrite) IR spectroscopy was used. Figure 2 shows the FT-IR spectra of pure solids, cysteine and cystine, hematite, magnetite and ferrihydrite mixed for 24 h with artificial seawater at lower pH range and hematite, magnetite and ferrihydrite mixed for 24 h with artificial seawater plus cysteine (0.20 mol L^{-1}) at lower pH range. When the FT-IR spectrum of pure solid cysteine (Fig. 2A-a, B-a, C-a) was compared to the FT-IR spectra of cysteine adsorbed on hematite (Fig. 2A-d), magnetite (Fig. 2 B-d)and ferrihydrite (Fig. 2 C-d), the vanishing or shifting of several bands was observed. The bands at 1,140, 1,202, 1,223 and 1,742 cm^{-1} can be attributed to the NH_3^+ and CH_2

Fig. 1 Diffractograms of the samples: ferrihydrite, magnetite, hematite, ferrihydrite plus artificial seawater, magnetite plus artificial seawater, hematite plus artificial seawater, ferrihydrite plus artificial seawater plus Cys (0.20 mol L^{-1}), magnetite plus artificial seawater plus Cys (0.20 mol L^{-1}) and hematite plus artificial seawater plus Cys (0.20 mol L^{-1}). The samples were mixed in two different ranges of pH. *Cys* cysteine, *Cis* cystine, *Hal* seawater salts, *Mgt* magnetite, *Hem* hematite ▶

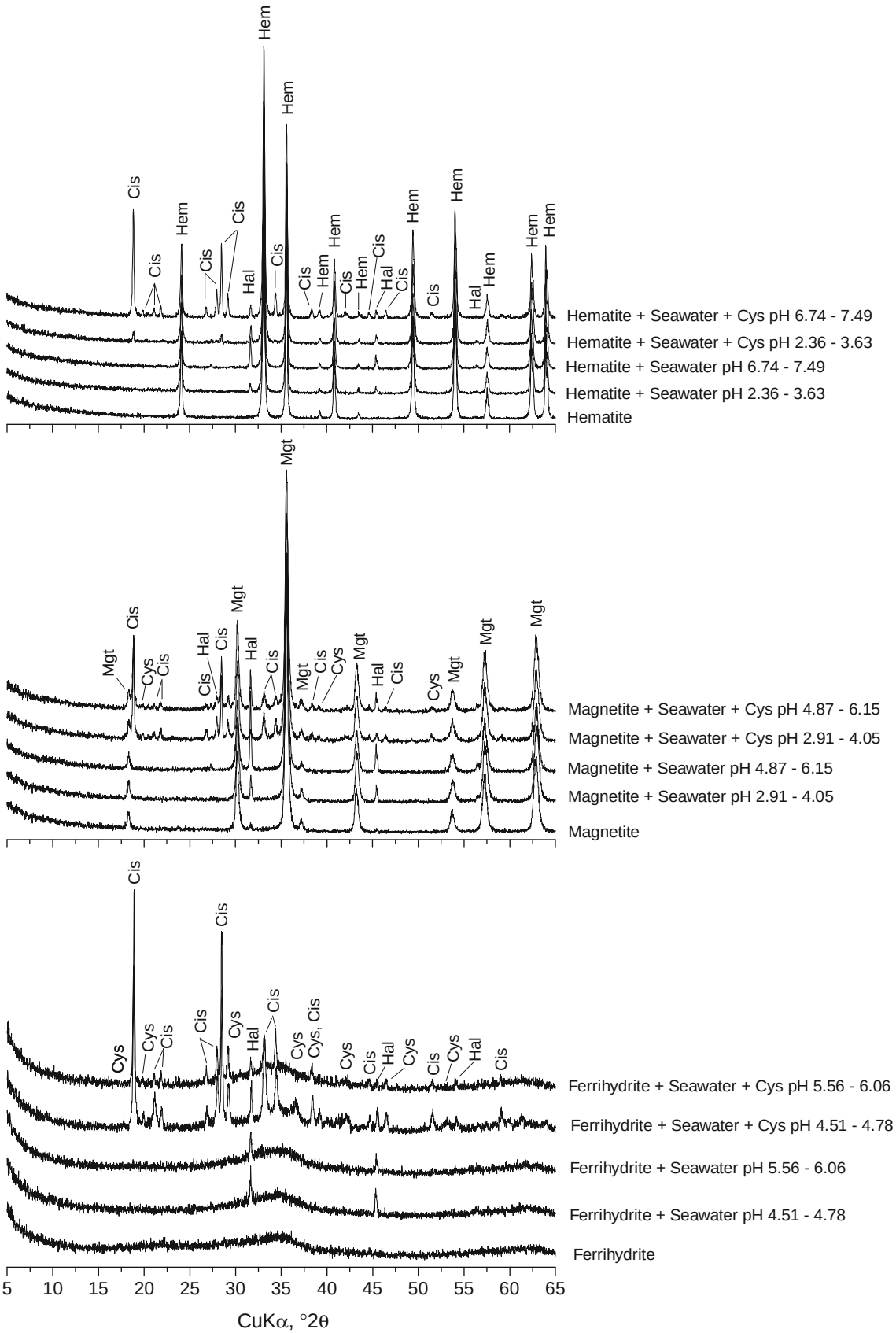
Hem
Cis
Hal
Mgt
Cys
Hematite + Seawater + Cys pH 6.74 - 7.49
Hematite + Seawater + Cys pH 2.36 - 3.63
Hematite + Seawater pH 6.74 - 7.49
Hematite + Seawater pH 2.36 - 3.63
Hematite
Magnetite + Seawater + Cys pH 4.87 - 6.15
Magnetite + Seawater + Cys pH 2.91 - 4.05
Magnetite + Seawater pH 4.87 - 6.15
Magnetite + Seawater pH 2.91 - 4.05
Magnetite
Ferrihydrite + Seawater + Cys pH 5.56 - 6.06
Ferrihydrite + Seawater + Cys pH 4.51 - 4.78
Ferrihydrite + Seawater pH 5.56 - 6.06
Ferrihydrite + Seawater pH 4.51 - 4.78
Ferrihydrite
5 10 15 20 25 30 35 40 45 50 55 60 65
CuKα, °2θ

Table 2 Amount of cysteine (μg) adsorbed on 100 mg of iron oxides

Iron oxides	Range of pH*	Net charge of iron oxides**	Net charge of Cys[#]	Amount adsorbed (μg)
Hematite	6.74–7.49	+	−	2601.3 ± 218.2^{b,d,i} (6)
	2.36–3.63	+	+	1984.9 ± 51.2^{b,d,f,h,j} (5)
Ferrihydrite	5.56–6.06	−	−	3205.3 ± 45.1^{c} (5)
	4.51–4.78	−/+	+	3206.2 ± 32.0^{a} (5)
Magnetite	4.87–6.15	+	−/+	2855.3 ± 74.4^{e} (5)
	2.91–4.05	+	+	2634.8 ± 170.6^{b,d,g} (6)

The results are presented as mean ± standard error of mean. The number of sets is given in parentheses with four samples each set. Cys (3,600 μg 5.0 mL^{-1}) was dissolved in artificial seawater as described in "Materials and methods". ANOVA test $F = 10.85$ and $p = 0.000$, SNK test ($p < 0.05$) a/b, c/d, e/f, g/h and i/j. Result *a* is statistically different from the results *b* with a confidence of 95% and same is valid for *c* and *d*, *e* and *f* and *i* and *j*

* The ranges of pH after the samples were tumbled for 24 h

** Based on the values of pH at point of zero charge (Table 1) and range of pH

[#] Based on range of pH and pH at point of isoelectric = 5.07

deformations, C–C(O)–O axial deformation and C=O stretching, respectively (Shindo and Brown 1965; Brigatti et al. 1999; Stewart and Fredericks 1999; Wolpert and Hellwig 2006). The hematite, magnetite and ferrihydrite samples with cysteine adsorbed on did not show the 2,562 cm^{-1} band attributed to the SH stretching vibration of cysteine (Figure not shown). Several authors also observed the vanishing of the 2,562 cm^{-1} band when they studied the interaction of cysteine with different minerals (Shindo and Brown 1965; Aryal et al. 2006; Benetoli et al. 2007; de Santana et al. 2010). The FT-IR spectrum of cystine showed bands at 539 and 650–672 cm^{-1} attributed to S–S and C–S stretching, respectively (Picquart et al. 1998; Wolpert and Hellwig 2006) and the same bands were observed for the samples of cysteine adsorbed on the iron oxides (Figure not shown). The adsorption of cysteine on iron oxides was also studied at higher pH range (Tables 1, 2) and the FT-IR spectra showed the same results as discussed before (spectra not shown). It should be pointed out that FT-IR spectra of the cystine and cysteine adsorbed on iron oxides are very similar (Fig. 2) and cystine was detected on the surface of iron oxides by X-ray diffractometry (Fig. 1). Amirbahman et al. (1997), Doong and Schink (2002), Benetoli et al. (2007), Cohen et al. (2008), Mantion et al. (2008) and de Santana et al. (2010) also obtained similar results when they studied the interaction of cysteine with several minerals containing Fe^{3+}. As shown in the reaction 1 these results are indicative that cysteine adsorbed on the iron oxides has been oxidized to cystine, thus Fe^{3+} was reduced to Fe^{2+}.

$$2Fe^{3+} + 2\text{cysteine} = 2Fe^{2+}\text{cystine} + 2H^{+} \quad (1)$$

A probable mechanism would involve: (1) adsorption of cysteine by the iron oxides through a ligand exchange reaction with the hydroxyls present on the ferrol (≡FeOH) surface functional group, (2) oxidation of the cysteine with electron transfer to the surface Fe^{3+}, and (3) Reduction of the Fe^{3+} from the iron oxide surface and formation of cystine. It should also be pointed out that after cystine is formed the FT-IR spectra reveal the vanishing of the 1,140, 1,223 and 1,742 cm^{-1} bands attributed to NH_3^+ deformation, C–C(O)–O axial deformation and C=O stretching. These changes could be indicating that cystine is coordinating with iron oxides through amine and carboxylic groups. However, Brigatti et al. 1999 attributed the vanishing the band at 1,760 cm^{-1} to low adsorption of cysteine species containing carboxylic group.

The iron oxides (hematite, magnetite, ferrihydrite) were mixed for 24 h in two different range of pH with artificial seawater plus cysteine. Afterwards these solutions were lyophilized and analyzed by infrared spectroscopy. In general, for both pH ranges the FT-IR spectra of the solutions (artificial seawater plus cysteine) mixed with hematite showed bands of solids, cysteine and cystine (Figure not shown). At lower pH range, the bands at 1,521 cm^{-1} (deformation NH_3^+) and 2,562 cm^{-1} (stretching S–H) were shifted to 1,512 and 2,542 cm^{-1}, respectively. The shifting of the 2,562 cm^{-1} band occurred probably because cysteine in the lyophilized sample is in the zwitterionic form (Pawlukojć et al. 2005). For both range of pH, the 1,746 cm^{-1} band that attributed to stretching C=O of cysteine was not observed in the lyophilized samples, probably because the carboxylic group is charged (Wolpert and Hellwig 2006). The bands at 1,521 cm^{-1} (deformation NH_3^+) and 2,562 cm^{-1} (stretching S–H) were not observed in the lyophilized sample at higher range of pH. In general, for magnetite and ferrihydrite, the FT-IR spectra of lyophilized solutions of artificial seawater plus cysteine are not similar to the FT-IR spectra of cysteine or cystine.

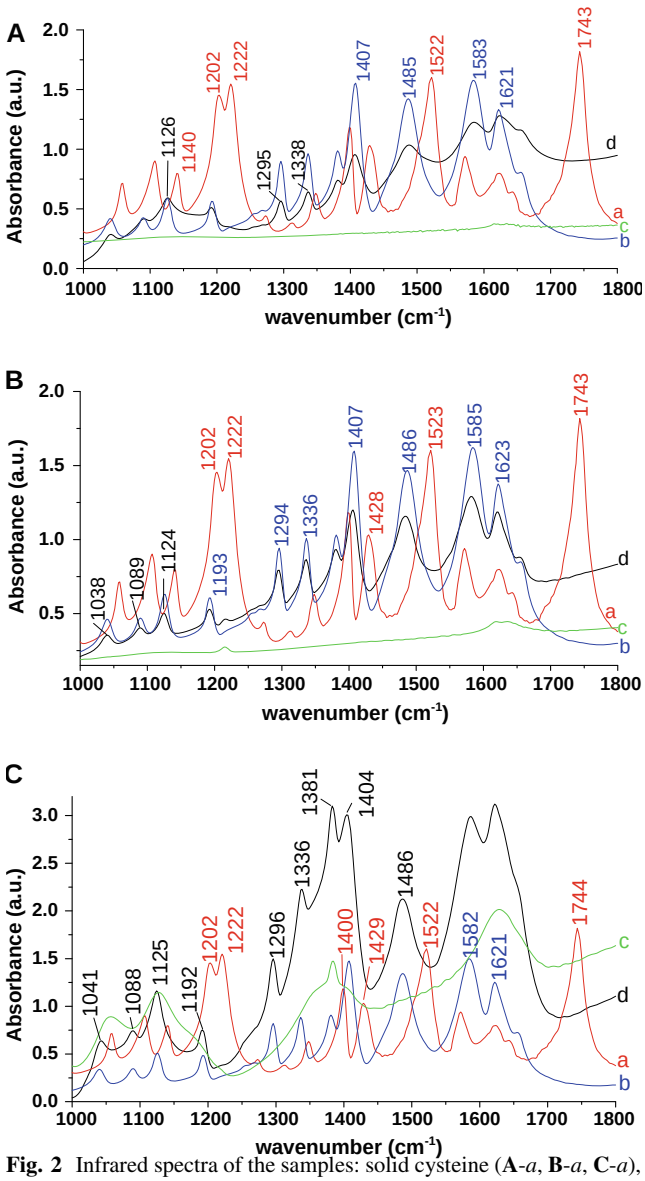

Fig. 2 Infrared spectra of the samples: solid cysteine (**A**-*a*, **B**-*a*, **C**-*a*), solid cystine (**A**-*b*, **B**-*b*, **C**-*b*), hematite (**A**-*c*), magnetite (**B**-*c*) and ferrihydrite (**C**–*c*) were mixed with artificial seawater for 24 h at lower pH and hematite (**A**-*d*), magnetite (**B**-*d*) and ferrihydrite (**C**-*d*) were mixed with artificial seawater plus cysteine (0.20 mol L^{-1}) for 24 h at lower pH. The samples were spun for 15 min at 2,000 rpm and were dried overnight at 60°C

After the iron oxides (hematite, magnetite, ferrihydrite) were mixed with artificial seawater plus cysteine (0.20 mol L^{-1}) for 24 h and dried overnight at 60°C, they were mixed for 24 h with KCl (0.10 mol L^{-1}) and dried overnight at 60°C. For both pH ranges, the FT-IR spectra of hematite and ferrihydrite did not change after these iron oxides were mixed with KCl and the spectra of cysteine adsorbed on these iron oxides are the same as cystine. For both pH ranges, the FT-IR spectra of magnetite showed all characteristic bands of cystine, however, in the region of 2,300–2,800 cm^{-1}, the FT-IR spectra showed several bands that are not showed in the FT-IR spectra of cysteine or cystine. The FT-IR spectra of all lyophilized samples of the KCl solution did not show the characteristic bands of cystine or cysteine (Figure not shown). Thus, the KCl solution did not desorb cystine/cysteine from the iron oxides. These results are in agreement with those obtained by de Santana et al. (2010), where a solution of KCl (1.0 mol L^{-1}) did not desorb cysteine from bentonite. Brigatti et al. (1999) studied desorption of cysteine from smectites enriched with Na^{+}, Ca^{2+} and Cu^{2+} and observed that desorption depends on the cation used and up to 50% of cysteine could be desorbed after 13 extraction with acidic water.

Figure 1 shows X-ray diffractograms of iron oxides (hematite, magnetite and ferrihydrite) without previous treatment, iron oxides mixed with artificial seawater for 24 h in two different ranges of pH and iron oxides mixed with artificial seawater plus cysteine (0.20 mol L^{-1}) for 24 h in two different ranges of pH. Original synthetic iron oxides did not transform to other minerals in the presence of artificial seawater and the cysteine independent of the solution pH. In the presence of artificial seawater, entrapped solution after drying out precipitated halite (NaCl). Peak positions and crystalographical attributes for all iron oxides were preserved. After adsorption, the X-ray diffractograms of the samples of cysteine also showed peaks of cysteine, cystine and artificial seawater salts (halite) in both ranges of pH (Fig. 1). Presence of cysteine and halite on X-ray diffractograms is an artifact of the samples treatment after the adsorption experiments and there is no evidence of any chemical relation between the iron oxides and these precipitates. However, for the cysteine adsorption treatment on hematite, the X-ray diffractograms show only diffraction peaks associated to artificial seawater salts and cystine, therefore, in this case, transformation of most cysteine to cystine (Eq. 1, above) (Fig. 1) was verified.

For magnetite and ferrihydrite, cysteine and cystine are present in the XRD patterns for the adsorption experiments (Lambert 2008) but the reaction does go to completeness as observed for hematite. XRD is not able to measure the amount of cystine formed from the oxidation of the cysteine and there is no possibility to confirm the fate of the Fe^{2+} produced, being adsorbed onto surface; oxidized and then adsorbed on the precursor minerals surface; form the same mineral or a secondary iron oxide which would not be identified by XRD due to its low concentration (<5%). Enlargement of Fig. 1 in the region 5°–30° showed the strongest peak for cysteine occurring at 18.24°2θ and for cystine at 28.56°2θ (Figure not shown), however, the peak of cysteine was not observed for the hematite samples. The affinity of cysteine to the hematite surface and complete oxidation to form cystine occurred independent of solution pH and is rather interesting since hematite presented the smallest specific surface area among the iron oxides and

Table 3 Resonance line intensities of Fe^{3+}

Iron oxides	Sample	Range of pH	Cys	Line 1 Fe^{3+} ($g = 7.5$)	Line 2 Fe^{3+} ($g = 3.8$)	Line 3 Fe^{3+} ($g \approx 2$)
Hematite	A	2.36–3.63	Without	1.0 ± 0.1	1.9 ± 0.1	23.5 ± 0.5
			With	1.9 ± 0.5	3.7 ± 0.9	14.3 ± 1.7
		6.74–7.49	Without	0.5 ± 0.5	1.0 ± 1.0	22.5 ± 1.5
			With	0.7 ± 0.2	1.4 ± 0.5	17.5 ± 5.5
	B (KCl)	2.36–3.63	Without	0.5 ± 0.5	0.9 ± 0.9	36.0 ± 25.0
			With	1.9 ± 0.5	3.8 ± 1.1	14.8 ± 1.8
		6.74–7.49	Without	1.3 ± 1.3	2.5 ± 2.5	31.8 ± 1.8
			With	0.4 ± 0.4	0.4 ± 0.4	22.0 ± 1.0
Ferrihydrite	A	4.51–4.78	Without	–	–	2.9 ± 0.4
			With	–	–	3.4 ± 0.2
		5.56–6.06	Without	–	–	3.4 ± 0.1
			With	–	–	3.2 ± 0.2
	B (KCl)	4.51–4.78	Without	–	–	3.1 ± 0.7
			With	–	–	1.6 ± 0.6
		5.56–6.06	Without	–	–	4.6 ± 0.1
			With	–	–	2.3 ± 0.3

The results are presented as mean ± standard error of mean. All results are mean of two analyses. The results of resonance line intensities of Fe^{3+} of samples A were obtained in two ranges of pH 2.36–3.63 and 6.74–7.49, 4.51–4.78 and 5.56–6.06 for hematite and ferrihydrite, respectively, after the samples were mixed for 24 h with artificial seawater and artificial seawater plus cysteine (0.20 mol L^{-1}). For the samples B, after they were through the process of A, the iron oxides were mixed for 24 h with KCl (0.10 mol L^{-1})

should have less reactivity for the amino acid in solution. The FT-IR spectra did not detect cysteine on the iron oxides probably because the characteristic band (2,562 cm^{-1}) of cysteine is weak. Mantion et al. (2008) studied the synthesis of several iron oxides in the presence of amino acids. When the iron oxides were synthesized in the presence of cysteine, the X-ray diffractograms showed cystine on them; however, the authors did not report the presence of cysteine.

Table 3 shows the results of EPR spectroscopy of the samples of hematite and ferrihydrite mixed with artificial seawater and artificial seawater plus cysteine (0.20 mol L^{-1}) in two different ranges of pH as well as the same samples after they were mixed with KCl (0.10 mol L^{-1}). EPR spectra were not obtained for the samples of magnetite because this iron oxide showed a strong absorption of microwave in region that the spectra were recorded, impairing the measurement of these samples. The EPR spectra show three resonance lines $g = 7.5$, $g = 3.8$ and $g \approx 2$. The resonance line $g \approx 2$ showed the highest intensity as expected since hematite and ferrihydrite are iron oxides and this line is due to hydroxides and oxides of Fe^{3+} (Guskos et al. 2002; Carbone et al. 2005; Mota et al. 2009). For hematite samples, in both pH, the intensity of the resonance line $g \approx 2$ decreased when samples of artificial seawater plus cysteine were compared to the samples treated only with artificial seawater (Table 3). The same results were observed for the samples of hematite and ferrihydrite with and without cysteine that were mixed with KCl (Table 3). De Santana et al. (2010) also obtained similar results when they studied the adsorption of cysteine on bentonite and montmorillonite. However, the intensity of the resonance line $g \approx 2$ did not change for the samples of ferrihydrite with artificial seawater and artificial seawater plus cysteine (Table 3). The resonance line $g = 3.8$ could be related to Fe^{3+} with rhombic symmetry as well as the interaction of Fe^{3+} with organic matter, this line is very common in soils (Guskos et al. 2002; Carbone et al. 2005; Mota et al. 2009). Since resonance line $g = 3.8$ is due to interaction of Fe^{3+} with organic matter, in general this line was higher in the samples with cysteine than without cysteine (Table 3). The resonance line $g = 7.5$ showed a similar change as observed for resonance line $g = 3.8$ (Table 3). For the resonance lines $g = 3.8$ and $g = 7.5$, de Santana et al. (2010) obtained the same results when they studied the adsorption of cysteine on bentonite and montmorillonite.

Table 4 shows Mössbauer hyperfine parameters and subspectral areas of iron oxides (hematite, magnetite, ferrihydrite) without previous treatment, mixed with artificial seawater, mixed with artificial seawater plus cysteine (0.20 mol L^{-1}). All the samples without any previous treatment show hyperfine parameters consistent with earlier reported values, including the $Fe^{2+,3+}/Fe^{3+}$ ratio for magnetite (Schwertmann and Cornell 1991; Wade et al. 1999; Kosmulski et al. 2003). Further treatments (artificial seawater plus cysteine) did not significantly change the hyperfine parameters of any iron oxide. However, a large

Table 4 Mössbauer hyperfine parameters and subspectral areas for the iron oxides, without any previous treatment and treated in two different ranges of pH, without/with cysteine adsorbed on

Iron Oxide	pH	Subspectrum	IS (mm/s) (±0.02)	QS (mm/s) (±0.02)	B_{hf} (T) (±1.1)	Γ (mm/s) (±0.02)	Área (%) (±0.3)
Hematite	–	Sextet (Fe^{3+})	0.37	−0.22	51.3	0.29	100
	2.36–3.63	Sextet (Fe^{3+})	0.37/0.37	−0.20/−0.20	51.8/51.8	0.32/0.28	100
	6.74–7.49	Sextet (Fe^{3+})	0.37/0.37	−0.20/−0.20	51.6/51.8	0.37/0.32	100
Ferrihydrite	–	Sextet (Fe^{3+})	0.34	0.68	–	0.46	100
	4.51–4.78	Doublet (Fe^{3+})	0.34/0.35	0.72/0.70	–	0.47/0.47	100
	5.56–6.06	Doublet (Fe^{3+})	0.35/0.34	0.72/0.67	–	0.47/0.52	100
Magnetite	–	Sextet (Fe^{3+})	0.30	−0.02	48.5	0.39	33
		Sextet ($Fe^{3+,2+}$)	0.54	−0.05	45.4	0.99	67
	2.91–4.05	Sextet (Fe^{3+})	0.32/0.32	0.03/0.02	48.0/48.0	0.59/0.57	61/54
		Sextet ($Fe^{3+,2+}$)	0.51/0.51	0.05/0.09	44.5/44.4	0.86/0.97	39/46
	4.87–6.15	Sextet (Fe^{3+})	0.32/0.32	−0.20/0.03	48.0/47.8	0.61/0.59	61/59
		Sextet ($Fe^{3+,2+}$)	0.57/0.53	−0.04/0.05	44.3/44.1	0.85/0.93	39/41

IS isomer shift, *QS* quadrupole splitting, B_{hf} hyperfine magnetic field

decrease in the $Fe^{2+,3+}$ subspectral area was observed for magnetite mixed with artificial seawater and artificial seawater plus cysteine. Mantion et al. (2008) showed that concentration as low as 1.0 mmol L^{-1} of cysteine prevent the synthesis of magnetite. The results of Table 4 show that the formation of Fe^{2+} did not occur, or if was formed immediately oxidized to Fe^{3+}. This is probably what happened since; FT-IR spectroscopy data showed formation of cystine for all iron oxides, thus Fe^{2+} should be formed. Benetoli et al. (2007) and de Santana et al. (2010) showed that if cysteine and thiourea were adsorbed on bentonite and montmorillonite, an increase in the Fe^{2+} was observed by Mossbauer spectroscopy but this reduction occurs inside the structure of the clay minerals, and even though this destabilize their charge balance, enhancing weathering (Sposito 1989), it was not able to produce redox reactions because the oxygen dissolved in the seawater would not be affected. But for the iron oxides, in this experiment, exposed ferrol surface functional group are more susceptible to the redox process. Thus, cysteine was adsorbed on the iron oxides generating Fe^{2+} that was released to the solution and oxidized to Fe^{3+} by the oxygen present in the artificial seawater. The reduction of cystine by Fe^{2+} generating cysteine and Fe^{3+} is another possibility worth further investigation, since Doong and Schink (2002) showed this reaction occurred besides the rate of formation of Fe^{3+} and cysteine was low.

Conclusion

The specific surface area and pH at point of zero charge of the iron oxides were influenced by mixing them with seawater or seawater plus cysteine.

Ferrihydrite was the iron oxide featuring most adsorbed cysteine ($p < 0.05$). The pH has an effect only in adsorption of cysteine on hematite ($p < 0.05$).

The results of FT-IR spectroscopy showed the formation of cystine and proved that KCl did not desorb cystine from the iron oxides.

X-ray diffractometry showed no change on the iron oxides mineralogy but the formation of cystine from the oxidation of cysteine in all three synthetic minerals.

The oxidation reaction cysteine → cystine was more pronounced with the hematite mineral, which has the smallest specific surface area.

The EPR spectroscopy showed that cysteine interacts with iron oxides changing the relative amounts of oxides and hydroxide of iron.

The Mössbauer spectroscopy did not show the formation of Fe^{2+}. An explanation is that Fe^{2+} was oxidized by the oxygen. Another possible explanation is the reduction of cystine by Fe^{2+} generating cysteine and Fe^{3+}.

Cystine synthesized remains adsorbed on the surface of iron oxides and the amine and carboxylic group are involved in this interaction.

Acknowledgments This research was supported by grant from Fundação Araucária (15279). The authors are grateful to Dr. Antonio A. da Silva Alfaya for the suggestions and discussion when the manuscript was being prepared.

References

Amirbahman A, Sigg L, von Gunten U (1997) Reductive dissolution of Fe(III) (hydr) oxides by cysteine: kinetics and mechanism. J Colloid Interface Sci 194:194–206

Aryal S, Remant BKC, Dharmaraj N, Bhattarai N, Kim CH, Kim HY (2006) Spectroscopic identification of S–Au interaction in cysteine capped gold nanoparticles. Spectrochimica Acta Part A 63:160–163

Baalousha M (2009) Aggregation and disaggregation of iron oxide nanoparticles: influence of particle concentration, pH and natural organic matter. Sci Total Environ 407:2093–2101

Basiuk VA (2002) Adsorption of biomolecules at silica. Encyclopedia of surface and colloid science. Marcel Dekker Inc., New York, pp 277–293

Basiuk VA, Gromovoy TY (1996) Comparative study of amino acid adsorption on bare and octadecyl silica from water using high performance liquid chromatography. Colloids Surf A Physicochem Eng Asp 118:127–140

Baumgartner E, Blesa MA, Maroto AJG (1982) Kinetics of the dissolution of magnetite in thioglycolic acid solutions. J Chem Soc Dalton Trans 9:1649–1654

Bebié J, Schoonen MAA (2000) Pyrite surface interaction with selected organic aqueous species under anoxic conditions. Geochem Trans 1:47–53

Benetoli LO, de Souza CM, da Silva KL, de Souza Junior IG, de Santana H, Paesano A Jr, Costa AC, Zaia CTBV, Zaia DAM (2007) Amino acid interaction with and adsorption on clays: FT-IR and Mössbauer spectroscopy and X-ray diffractometry investigations. Orig Life Evol Biosph 37:479–493

Bernal JD (1951) The physical basis of life. Routledge and Kegan Paul Ltd., London

Bishop JL, Murad E (2002) Spectroscopic and geochemical analyses of ferrihydrite from springs in Iceland and applications to Mars. Geol Soc Lond Spec Publ 202:350–370

Brigatti MF, Luoli C, Montorsi S, Poppi L (1999) Effects of exchange cations and layer-charge location on cysteine retention by smectites. Clays Clay Miner 47:664–667

Brunauer S, Emmett PH, Teller E (1938) Adsorption of gases in multimolecular layers. J Am Chem Soc 60:309–319

Carbone C, di Benedetto F, Marescotti P, Sangregorio C, Sorace L, Lima N, Romanelli M, Luchetti G, Cipriani C (2005) Natural Fe-oxide and -oxyhydroxide nanoparticles: na EPR and SQUID investigation. Mineral Petrol 85:19–32

Catling DC, Moore JM (2003) The nature of course-grained crystalline hematite and its implications for the early environment of Mars. Icarus 165:277–300

Cohen H, Gedanken A, Zhong Z (2008) One step synthesis and characterization of ultrastable and amorphous Fe_3O_4 colloids capped with cysteine molecules. J Phys Chem C 112:15429–15438

Darnell J, Lodish H, Baltimore D (1990) Molecular cell biology. Scientific American Books, New York

de Santana H, Paesano A Jr, da Costa AC, Di Mauro E, de Souza Junior IG, Ivashita FF, de Souza CM, Zaia CTBV, Zaia DAM (2010) Cysteine, thiourea and thiocyanate interactions with clays: FT-IR, Mossbauer and EPR spectroscopy and X- ray diffractometry. Amino Acids 38:1089–1099

Doong RA, Schink B (2002) Cysteine- mediated reductive dissolution of poorly crystalline iron(III) oxides by *Geobacter sulfurreducens*. Environ Sci Technol 36:2939–2945

Faivre D, Zuddas P (2006) An integrated approach for determining the origin of magnetite nanoparticles. Earth Planet Sci Lett 243:53–60

Guskos N, Papadopoulos GJ, Likodimos V, Patapis S, Yarmis D, Przepiera A, Przepiera K, Majszczyk J, Typek J, Wabia M, Aidinis K, Drazek Z (2002) Photoacoustic, EPR and electrical conductivity investigations of three synthetic mineral pigments: hematite, goethite and magnetite. Mater Res Bull 37:1051–1061

Kosmulski M, Maczka E, Jartych E, Rosenholm JB (2003) Synthesis and characterization of goethite and goethite-hematite composite: experimental study and literature survey. Adv Colloid Interface Sci 103:57–76

Lahav N, Chang S (1976) The possible role of solid surface area in condensation reactions during chemical evolution: reevalution. J Mol Evol 8:357–380

Lambert JF (2008) Adsorption and polymerization of amino acids on minerals surfaces: a review. Orig Life Evol Biosph 38:211–242

Li L, Stanforth R (2000) Distinguishing adsorption and surface precipitation of phosphate on goethite (α-FeOOH). J Colloid Interface Sci 230:12–21

Mantion A, Gozzo F, Schmitt B, Stern WB, Gerber Y, Robin AY, Fromm KM, Painsi M, Taubert A (2008) Amino acids in iron oxide mineralization: (incomplete) crystal phase selection is achieved even with single amino acids. J Phys Chem C 112:12104–12110

Marti EM, Methivier Ch, Pradier CM (2004) (*S*)-cysteine chemisorptions on Cu (110), from the gas or liquid phase: an FT-RAIRS and XPS study. Langmuir 20:10223–10230

Matrajt G, Blanot D (2004) Properties of synthetic ferrihydrite as an amino acid adsorbent and a promoter of peptide bond formation. Amino Acids 26:153–158

Mota L, Toledo R, Faria RT Jr, da Silva EC, Vargas H, Deladillo-Hotfort I (2009) Thermally treated soli clays as ceramic raw materials: characterization by x-ray diffraction, photoacoustic spectroscopy and electron spin resonance. Appl Clay Sci 43:243–247

Pawlukojć A, Leciejewicz J, Ramirez-Cuesta AJ, Nowicka-Scheibe J (2005) L-Cysteine: neutron spectroscopy, Raman, IR and ab initio study. Spectrochimica Acta part A 61:2474–2481

Picquart M, Abedinzadeh Z, Grajcar L, Baron MH (1998) Spectroscopic study of *N*-acetylcysteine and *N*-acetylcistine/hydrogen peroxide complexation. Chem Phys 228:279–291

Rietmeijer FJM (1996) The ultrafine mineralogy of a molten interplanetary dust particle as an example of the quench regime of atmospheric entry heating. Meteorit Planet Sci 31:237–242

Schwertmann U, Cornell RM (1991) Iron oxides in the laboratory—preparation and characterization. Verlagsgesells chat, Weinheim, p 137

Shindo H, Brown TL (1965) Infrared spectra of complexes of L-cysteine and related compounds with zinc (II), cadmium (II), mercury (II) and lead (II). J Am Chem Soc 87:1904–1909

Sposito G (1989) The chemistry of soil. Oxford University Press, New York, p 277

Stewart S, Fredericks PM (1999) Surface-enhanced Raman spectroscopy of amino acids adsorbed on electrochemically prepared silver surface. Spectrochimica Acta Part A 55:1641–1660

Uehara G (1979) Mineral–chemical properties of oxisols. International Soil Classification Workshop, vol 2. Soil Survey Division—Land Development Department, Bangkok, Malaysia, pp 45–60

Wade ML, Agresti DG, Wdowiak TJ, Armendarez LP (1999) A Mössbauer investigation of iron rich terrestrial hydrothermal vent systems: lessons for Mars exploration. J Geophys Res 104:8489–8507

Wolpert M, Hellwig P (2006) Infrared spectra and molar absorption coefficients of the 20 alpha amino acids in aqueous solutions in the spectral range from 1800 to 500 (cm^{-1}). Spectrochimica Acta part A 64:987–1001

Zaia DAM (2004) Review of adsorption of amino acids on minerals: was it important for origin of life. Amino Acids 27:113–118

Zaia DAM, Ribas KC, Zaia CTBV (1999) Spectrphotometric determination of cysteine and: or carbocysteine in a mixture of amino acids, shampoo, and pharmaceutical products using *p*-benzoquinone. Talanta 50:1003–1010

Zaia DAM, Zaia CTBV, de Santana H (2008) Which amino acids should be used in prebiotic chemistry studies? Orig Life Evol Biosph 38:469–488